INVESTIGATION OF REACTOR CONDITION MONITORING AND SINGULARITY DETECTION VIA WAVELET TRANSFORM AND DE-NOISING

OK JOO KIM[1], NAM ZIN CHO[1*], CHANG JE PARK[2], and MOON GHU PARK[3]
[1] Department of Nuclear and Quantum Engineering, Korea Advanced Institute of Science and Technology
373-1 Guseong-dong, Yuseong-gu, Daejeon 305-701, Korea
[2] Korea Atomic Energy Research Institute
150 Deokjin-dong, Yuseong-gu, Daejeon 305-353, Korea
[3] Korea Electric Power Research Institute
103-16 Munji-dong, Yuseong-gu, Daejeon 305-380, Korea
[*]Corresponding author. E-mail : nzcho@kaist.ac.kr

Received December 28, 2006
Accepted for Publication April 14, 2007

Wavelet theory was applied to detect a singularity in a reactor power signal. Compared to Fourier transform, wavelet transform has localization properties in space and frequency. Therefore, using wavelet transform after de-noising, singular points can easily be found. To test this theory, reactor power signals were generated using the HANARO (a Korean multi-purpose research reactor) dynamics model consisting of 39 nonlinear differential equations contaminated with Gaussian noise. Wavelet transform decomposition and de-noising procedures were applied to these signals. It was possible to detect singular events such as a sudden reactivity change and abrupt intrinsic property changes. Thus, this method could be profitably utilized in a real-time system for automatic event recognition (e.g., reactor condition monitoring).

KEYWORDS : De-noising by Thresholding Algorithm, Singularity Detection, Wavelet Transform, HANARO Research Reactor

1. INTRODUCTION

Wavelets are useful in many different fields of science and engineering. Examples include sound analyses, decomposition and reconstruction of visual data, and detections of edges and singularities [1,2]. In addition, several researchers have tried to solve differential equations using orthonormal wavelet functions [3], including the neutron diffusion equation [4,5] and neutron transport equation [6].

In this paper, the focus is on the detection of singularities for processing signals using the wavelet theory. It is well known that the neutron noise theory allows monitoring and diagnosis of many reactor operating parameters and conditions. The neutron noise theory has been used for diagnostic purposes, for the identification of abnormal situations and for the estimation of dynamical core parameters when the reactor is at steady-state conditions. Many previous works can be found in the literature, and more can be found in the references therein [7,8,9,10]. In recent years, applications of soft computing and artificial intelligence techniques has drawn particular attention [11,12,13]. Over the past several decades, many significant contributions to the neutron noise theory have been reported. Most of these studies are based on the frequency domain and most address the signals at steady-state conditions, but the techniques can be used successfully for diagnoses of many practical systems. In this work, the primary concern is on the diagnoses of parameter changes in nuclear reactors with the time-domain approach using wavelet theory. First, the de-noising capability of the wavelet transform is exploited to make plant signal smoother and more readable. Second, method of detecting abrupt changes in a dynamics system is investigated. The method is then applied to a research-reactor dynamics model. In this work, the orthonormal basis of compactly supported wavelets constructed by Daubechies [1] is used.

2. WAVELET THEORY

One of the important features of wavelets is a *multi-resolution analysis* (*MRA*). This enables the construction of a hierarchy of approximations to functions in various subspaces. An MRA of $L^2(R)$ is defined as a set of closed subspaces V_j with $j \in Z$ that exhibit the following

properties:

1) $V_j \subset V_{j+1}$,
2) $\nu(x) \in V_j \Leftrightarrow \nu(2x) \in V_{j+1}$ and $\nu(x) \in V_0 \Leftrightarrow \nu(x+1) \in V_0$,
3) $\bigcup_{j=-\infty}^{+\infty} V_j$ is dense in L^2 (R) and $\bigcap_{j=-\infty}^{+\infty} V_j = \{0\}$,
4) A scaling function $\phi(x) \in V_0$ exists such that the set $\{\phi(x-l) \mid l \in Z\}$ is the basis of V_0.

Consequently, the sequence $(h_k) \in l^2(Z)$ exists such that the scaling function satisfies the *two-scale difference equation*

$$\phi(x) = \sqrt{2} \sum_k h_k \phi(2x-k). \tag{1}$$

The set of functions $\{\phi_{j,l}(x) \mid l \in Z\}$ with $\phi_{j,l}(x) = 2^{j/2} \phi(2^j x - l)$ is the orthonormal basis of V_j.

The complementary space of V_j in V_{j+1} is denoted by W_j; that is $V_{j+1} = V_j \oplus W_j$. This satisfies following properties:

1) $W_k \perp W_l$ if $k \neq l$
2) $w(x) \in W_j \Leftrightarrow w(2x) \in W_{j+1}$ and $w(x) \in W_0 \Leftrightarrow w(x+1) \in W_0$,
3) $\bigoplus_{j=-\infty}^{+\infty} W_j = L^2(\mathrm{R})$,
4) A function $\psi(x) \in W_0$ exists such that the set $\{\psi(x-l) \mid l \in Z\}$ is the basis of W_0.

A function $\psi(x)$ is termed a mother wavelet. As the mother wavelet is also an element of V_1, the sequence $(g_k) \in l^2(Z)$ exists such that

$$\psi(x) = \sqrt{2} \sum_k g_k \phi(2x-k). \tag{2}$$

The set of functions $\{\psi_{j,l}(x) \mid l \in Z\}$ with $\psi_{j,l}(x) = 2^{j/2} \psi(2^j x - l)$ is the orthonormal basis of W_j. The Daubechies coefficients h_k and g_k are related by

$$g_k = (-1)^k h_{2N-1-k}, \tag{3}$$

where N is the Daubechies order.

In this study, fast wavelet transform (FWT) [14] is used to de-noise the signal and to detect the singularities. Assuming that a finite sequence s_k^0, $k = 1,2,...K$, is given, the FWT of this sequence can then be written as:

$$s_k^j = \sum_{n=0}^{2N-1} h_n s_{n+2k-1}^{j-1}, \tag{4}$$

$$d_k^j = \sum_{n=0}^{2N-1} g_n s_{n+2k-1}^{j-1}, \tag{5}$$

and the inverse fast wavelet transform (IFWT) can be written as:

$$s_{2n}^{j-1} = \sum_{k=1}^{N} h_{2k-1} s_{n-k+1}^j + \sum_{k=1}^{N} g_{2k-1} d_{n-k+1}^j, \tag{6}$$

$$s_{2n-1}^{j-1} = \sum_{k=1}^{N} h_{2k-2} s_{n-k+1}^j + \sum_{k=1}^{N} g_{2k-2} d_{n-k+1}^j. \tag{7}$$

FWT is a decomposition process of the original sequence. The original sequence is decomposed into approximation coefficients (s^j) and detail coefficients (d^j). The approximation coefficients contain low-frequency information and the detail coefficients have high-frequency information such as edges or discontinuities. The approximation coefficients become input signals recursively to the next-stage transform. Reversely, IFWT is a reconstruction process. Fig. 1 shows the decomposition and reconstruction processes of FWT and IFWT.

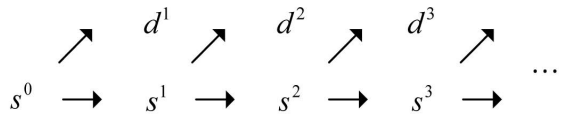

(a). Decomposition Process of FWT

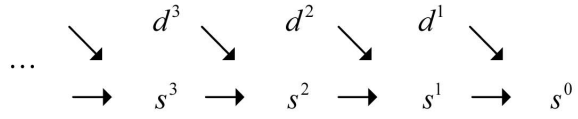

(b). Reconstruction Process of IFWT.

Fig. 1. Schematic Diagram of the Fast Wavelet Transform (FWT) and Inverse Fast Wavelet Transform (IFWT)

3. DE-NOISING USING THE THRESHOLDING ALGORITHM

In addition to the advantages related to its multi-resolution properties, the wavelet transform shows another important characteristic that can be exploited in the signal domain. This is the capability of discriminating a typical "noise" process from a typical "signal" process.

The de-noising capability is based on the different evolution across the scales of the detail coefficients (d^j) maxima, depending on the signal regularity degree, defined in terms of the Lipschitz exponent [15]. The detail coefficient maxima that have negative Lipschitz exponents tend to vanish as the scale increases, whereas this does not happen if the maxima are characterized by positive exponents. Fortunately, fluctuating noise causes negative Lipschitz exponents in the signal; therefore, it is possible to remove the noise from the corrupted signal by rejecting maxima whose Lipschitz exponents are negative. To select these maxima, thresholding algorithm can be used [16]. For a signal whose size is n, the threshold level (t) is given by

$$t = \sqrt{2\log(n)}\sigma \tag{8}$$

Where σ is the noise level of the signal. A simple choice for the threshold value is based on the idea of "de-noising", which attempts to eliminate pure noise terms. For white noise, σ can be estimated very well, for example by a robust scale estimate applied to the finest scale wavelet coefficients. Hence, it is assumed that σ is known. Assuming the noise is Gaussian allows the use of the property that for X_1,..., X_n *i.i.d.* $N(0, \sigma^2)$.

$$P(\max_{i=1,\cdots,n}|X_i| \le \sqrt{2\log(n)}\sigma) \to 1 \text{ as } n \to \infty. \tag{9}$$

Hence, the threshold $\sqrt{2\log(n)}\sigma$ will zero out for every term that has all noise and no signal components.

To de-noise the signal using the wavelet thresholding method, the following procedure is used:

First, the wavelet transform of the noisy signal is performed. Wavelet coefficients s and d are then obtained.

Secondly, detail coefficients d are passed through the thresholding function. There can be two choices: hard or soft thresholding. The *hard-thresholding* function and *soft-thresholding* function are, respectively [16],

$$T_{hard}(x;t) = xI, \quad (|x| > t), \tag{10}$$

$$T_{soft}(x;t) = \mathrm{sgn}(x)(|x| - t)I, \quad (|x| > t), \tag{11}$$

Where I is the usual indicator function. While the hard-thresholding preserves values that are greater than t and sets the others to equal zero (keep-or-kill), the soft-thresholding shrinks all the values by t towards zero (shrink-or-kill). This shrinking has the effect of reducing variance while increasing bias. While d is passed through the thresholding function, s is unchanged.

Lastly, the signal is reconstructed from s and the thresholded d by inverse wavelet transform, providing the de-noised signal.

4. SINGULARITY DETECTION

Essentially, the idea underlying most singularity-detection techniques is the computation of a local derivative operator. The wavelet-based method uses the fast wavelet transform.

The presence of noise makes the wavelet transform decomposition difficult if applied directly to the signal detection. However, the wavelet transform coefficients are able to localize the sharp variation points of a signal (and in particular the onset of anomaly) effectively, provided that the signal is de-noised, as was demonstrated by the application of the technique on synthetic data [15].

Assuming that the integral of a smoothing function $\theta(x)$ is equal to 1 and that it converges to 0 at infinity, if a wavelet $\psi(x)$ is equal to the first-derivative of a smoothing function $\theta(x)$, the wavelet function transform is computed by convolving the signal with a dilated wavelet. The wavelet transform of $f(x)$ at the scale s and position x, computed with respect to the wavelet $\psi(x)$, is defined by

$$W_s f(x) = f * \psi_s(x) = \int_{-\infty}^{\infty} f(u)\psi_s(x-u)du\,. \tag{12}$$

This can be easily derived [15] as

$$W_s^1 f(x) = f * (s\frac{d\theta_s(x)}{dx}) = s\frac{d}{dx}(f * \theta_s(x))\,. \tag{13}$$

The local extrema of $W_s^1 f(x)$ correspond to the inflection points of $f * \theta_s(x)$. For edge and singularity detection, only the local maxima of $|W_s^1 f(x)|$ are of interest. When detecting the local maxima of $|W_s^1 f(x)|$, the value of the wavelet transform is maintained at the corresponding location. It is noted that the regularity of the Daubechies wavelets increases linearly with N:

$\phi_{n,k}$, $\psi_{n,k} \in C^{\lambda(N)}$= space of Holder continuous functions with exponent $\lambda(N)$.

$$\begin{aligned} &\lambda(2) = 0.5500, \quad \lambda(3) = 1.08783, \\ &\lambda(4) = 1.67179, \quad , \lambda(N) = 0.3485N, \quad \text{for large } N. \end{aligned} \tag{14}$$

Therefore, the Daubechies wavelet $\psi(x)$ can be equal to the first-derivative of a smoothing function $\theta(x)$. One

signal sharp variation produces the detail coefficient maxima at the differing scales 2^j. The value of the detail coefficient maximum at scale 2^j measures the derivative of the signal smoothed at scale 2^j.

5. NUMERICAL TESTS

The wavelet thresholding method is applied to detect changes in the model parameters of HANARO, a multi-purpose research reactor in Korea. HANARO is cooled by ordinary water and moderated by heavy water. The reference plant model is simulated using a fifth-order Runge-Kutta method with adaptive time step sizes chosen to deal with the stiffness inherent in nuclear reactor dynamics. 39 nonlinear differential equations are used to describe the HANARO model [17]. The neutron kinetics part of the reactor dynamics is shown as follows:

1) Neutron flux in the core region:

$$\frac{dN_c}{dt} = \frac{1}{l_c}(\rho_0 + \rho_T + \rho_R - \beta - \gamma)N_c + \sum_{i=1}^{6}\lambda_i C_i + \frac{\alpha_{cr}}{l_c}N_r(t-\tau_{cr}) \quad (15)$$

2) Neutron flux in the reflector region:

$$\frac{dN_r}{dt} = \alpha_{rr}N_r + \sum_{j=1}^{9}\lambda_{Dj}D_j + \frac{\alpha_{rc}}{l_c}N_c(t-\tau_{rc}) \quad (16)$$

3) Delayed neutron precursors:

$$\frac{dC_i}{dt} = \frac{\beta_i}{l_c}N_c - \lambda_i C_i, \quad i = 1,...,6 \quad (17)$$

4) Photoneutron precursors:

$$\frac{dD_j}{dt} = \frac{\gamma_j}{l_c}N_c - \lambda_{Dj}D_j, \quad j = 1,...,9 \quad (18)$$

5) Reactivity feedback:

$$\rho_T = \alpha_c(T_c - T_{co}) + \alpha_f(T_f - T_{fo}) \quad (19)$$

6) Temperature of the fuel element:

$$\frac{dT_f}{dt} = \frac{1}{M_f C_f + M_{cl}C_{cl}}\left\{\eta_f Q_c - U_f A_f(T_f - T_c)\right\} \quad (20)$$

7) Temperature of the coolant passing through the reactor channels:

$$\frac{dT_c}{dt} = \frac{1}{M_c C_c}\left\{(1-\eta_f)Q_c + U_f A_f(T_f - T_c) - 2W_c C_c(T_c - T_l)\right\} \quad (21)$$

where

- A_f = heat transfer area of fuel
- C_c = specific hear of coolant water
- C_f = specific hear of fuel meat
- C_i = core-averaged *i*'th group precursor density
- D_j = reflector-averaged *j*'th group photoneutron precursor density
- M_c = mass of H_2O in coolant channel
- M_{cl} = mass of cladding
- M_f = mass of fuel
- N_c = core-aceraged neutron density (or reactor power)
- N_r = reflector-averaged neutron density
- Q_c = power produced in core
- T_c = core coolant temperature
- T_{co} = initial coolant temperature
- T_f = fuel element temperature
- T_{fo} = initial fuel temperature
- T_l = temperature in inlet
- U_f = heat transfer coefficient between fuel and core coolant
- W_c = core flow rate
- l_c = neutron generation time
- α_c = coolant temperature coefficient
- α_{cr}, α_{rc} = cross-coupling coefficients between core and reflector
- α_f = fuel temperature coefficient
- α_{rr} = coefficient of auto-coupling in reflector
- β_i = *i*'th group delayed neutron fraction ($\beta = \Sigma\beta_i$)
- γ_j = *j*'th group photoneutron fraction ($\gamma = \Sigma\gamma_i$)
- η_f = fraction of heat absorbed in fuel
- λ_i = *i*'th group delayed neutron decay constant
- λ_{Dj} = *j*'th group photoneutron decay constant
- ρ_R = external reactivity from control rod
- ρ_T = temperature feedback reactivity due to fuel and coolant temperature variation
- τ_{cr}, τ_{rc} = time lags for neutron transport

Here, the simulation time-step sizes are far smaller than the sampling time interval (Δt=0.01sec). Thus, the signals are piecewise constant in the plant simulation time steps. Normalized reactor power signals were generated with initial values of 1. A total of 128 simulated data are contaminated with the Gaussian noise $N(0,\sigma^2)$.

5.1 Change in the Reactivity [18]

The results with the Daubechies 3 wavelet are presented in Fig. 2. The reactivity is a series of step functions, as shown in Fig. 2(a). Fig. 2(b) and Fig. 2(e) are the results of reactivity changes with a Gaussian noise variance of $N(0,0.5^2)$ and $N(0,0.03^2)$ added to HANARO simulated

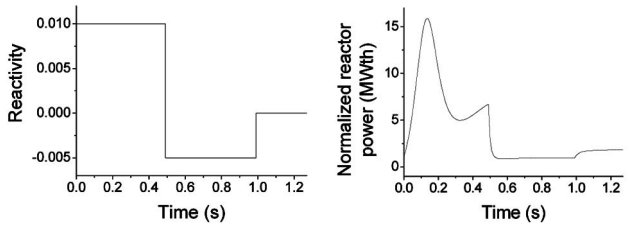

(a) Reactivity and Normalized Reactor Power

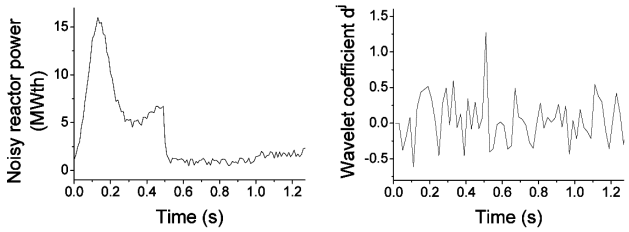

(b) Noisy Reactor Power and its Wavelet Coefficients d^1 (σ=0.5)

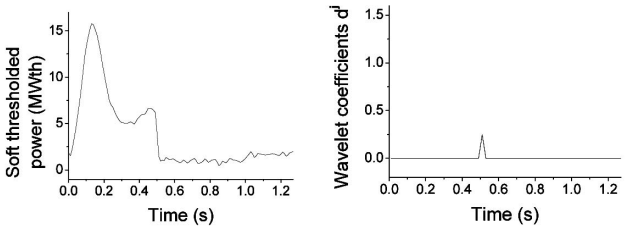

(c) Soft Thresholded Reactor Power and its Wavelet Coefficients d^1

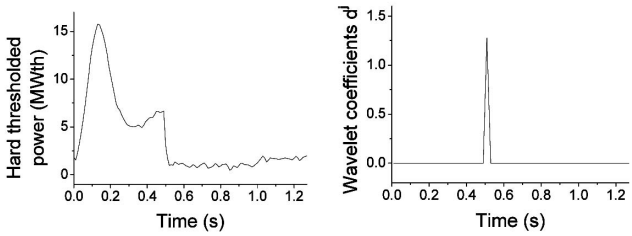

(d) Hard Thresholded Reactor Power and its Wavelet Coefficients d^1

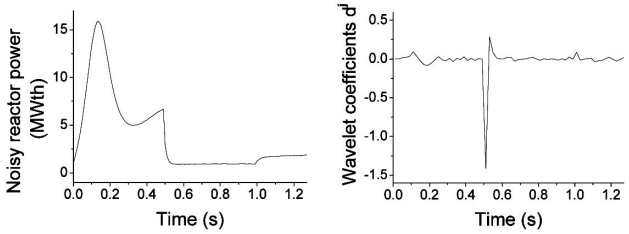

(e) Noisy Reactor Power and its Wavelet Coefficients d^1 (σ=0.03)

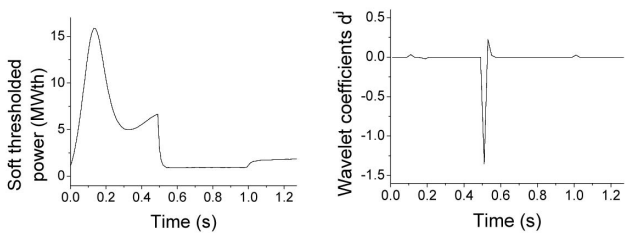

(f) Soft Thresholded Reactor Power and its Wavelet Coefficients d^1

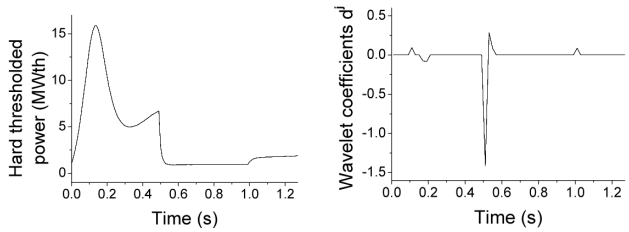

(g) Hard Thresholded Reactor Power and its Wavelet Coefficients d^1

Fig. 2. De-noised Reactor Power and its Wavelet Coefficients for the Daubechies 3 Wavelet

power, respectively. The root-mean-square error of each Daubechies wavelet is shown in Fig. 3. From the detail coefficients, it can be ascertained that abrupt change in the reactivity of the reactor have occurred. For σ=0.5, the reactivity change at t=0.5 sec is detected clearly, but the change at t=1.0 sec is buried in noise. For the second case of σ=0.03, the two reactivity changes are detected clearly.

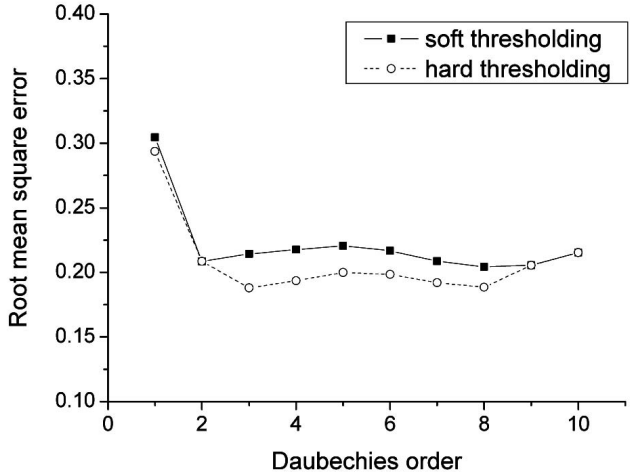

(a) σ = 0.5

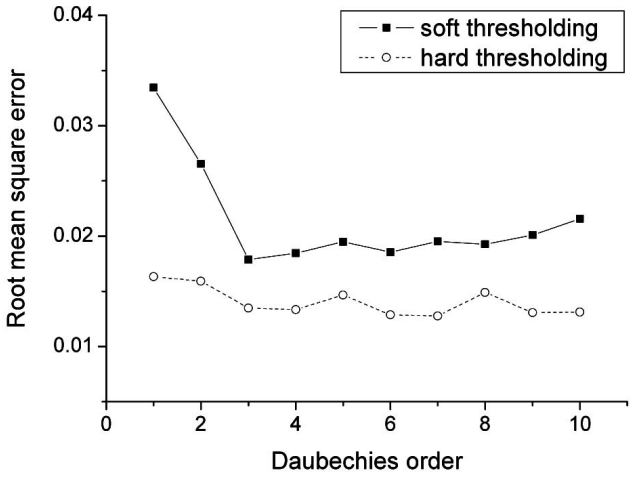

(b) $\sigma = 0.03$

Fig. 3. Root-mean-square Error of a De-noised Reactor Power With Soft and Hard Thresholding

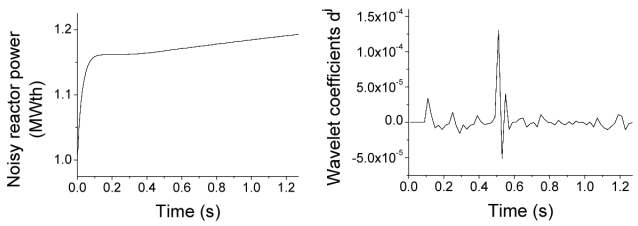

(b) Noisy Reactor Power and its Wavelet Coefficients d^1 (σ=10^{-5})

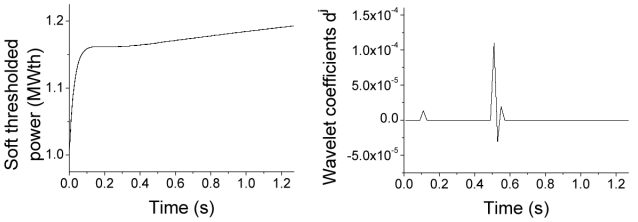

(c) Soft Thresholded Reactor Power and its Wavelet Coefficients d^1

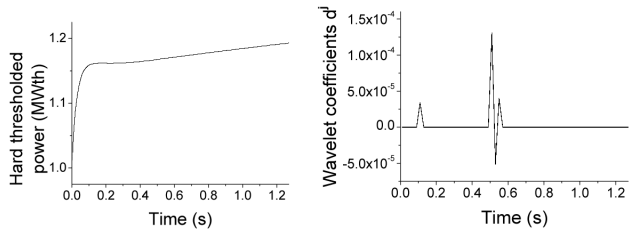

(d) Hard Thresholded Reactor Power and its Wavelet Coefficients d^1

Fig. 4. De-noised Reactor Power and its Wavelet Coefficients for the Daubechies 6 Wavelet

5.2 Change in the Neutron Generation Time (l_c)

5.2.1 Under Constant Reactivity

A constant reactivity ρ=0.001 is applied with a Gaussian noise of σ=10^{-5}. At t=0.5sec, the neutron generation time is reduced to one third of the initial value. This results in a very small increase of the reactor power. Normally, it is not easy to notice this small change by monitoring the reactor power. The result shows that the applied wavelet-based de-noising and decomposition procedure easily identifies the singular point in the detail coefficient. The result is shown in Fig. 4. The root-mean-square error of each Daubechies wavelet is presented in Fig. 5.

5.2.2 Under Fluctuating Reactivity

It was assumed that there exists a sinusoidal perturbation giving a reactivity fluctuation with a Gaussian noise of σ =10^{-5}. The neutron generation time is then decreased to one-third unexpectedly at t =0.5sec. This has a very small

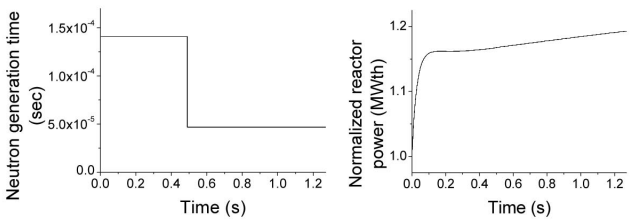

(a) Neutron Generation Time and Normalized Reactor Power

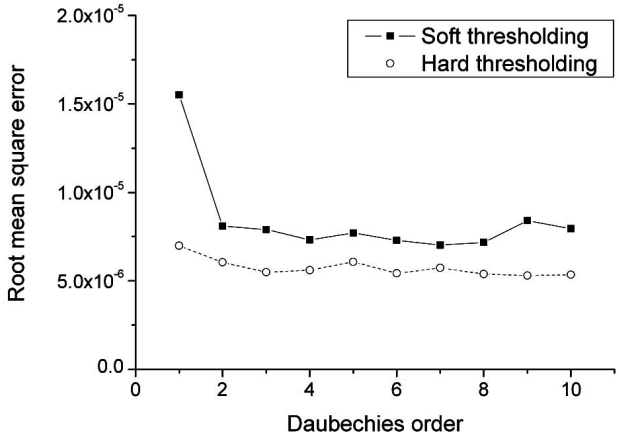

Fig. 5. Root-mean-square Error of a De-noised Reactor Power With Soft and Hard Thresholding

effect on the power level; hence, the power level continues to be dominated by fluctuating reactivity. From the detail coefficient by the Daubechies 6 wavelet, a significant change in the reactor state was found. The results are presented in Fig. 6 and Fig. 7.

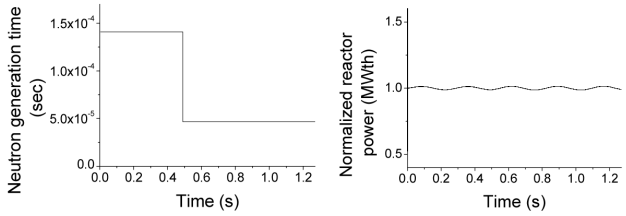

(a). Neutron Generation Time and Normalized Reactor Power

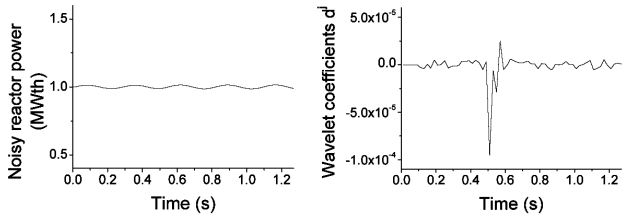

(b). Noisy Reactor Power and its Wavelet Coefficients d^1 (σ=10^{-5})

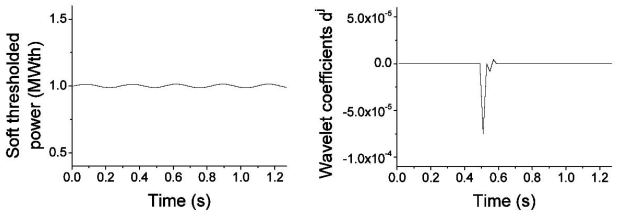

(c). Soft Thresholded Reactor Power and its Wavelet Coefficients d^1

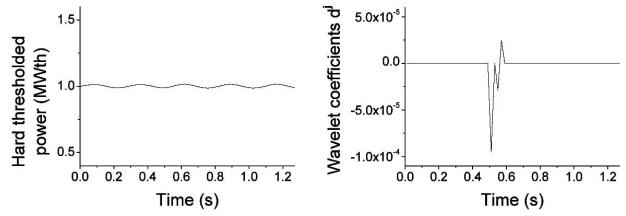

(d). Hard Thresholded Reactor Power and its Wavelet Coefficients d^1

Fig. 6. De-noised Reactor Power and its Wavelet Coefficients for the Daubechies 6 Wavelet

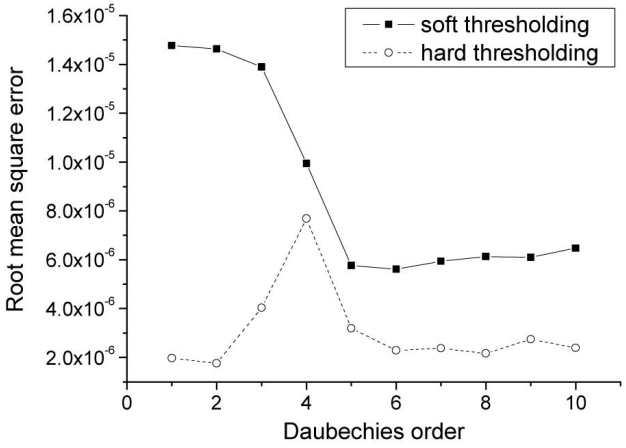

Fig. 7. Root-mean-square Error of a De-noised Reactor Power With Soft and Hard Thresholding

5.3 Change in the Delayed Neutron Fraction (β)

The power signal is generated via constant reactivity and the Gaussian noise $N(0,0.003^2)$. It is assumed that the delayed neutron fraction decreases to half of the initial value at $t=0.5$sec. The Daubechies 3 wavelet is used to perform the wavelet transform. the results are represented in Figs. 8 and 9.

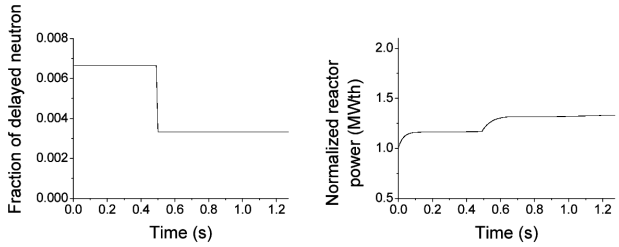

(a). Fraction of Delayed Neutron and Normalized Reactor Power

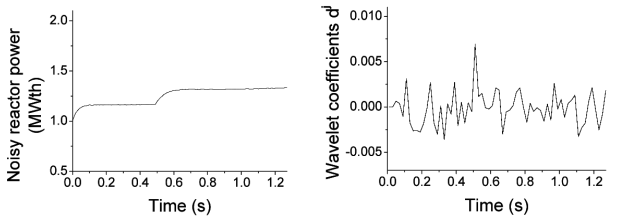

(b). Noisy Reactor Power and its Wavelet Coefficients d^1 (σ=0.003)

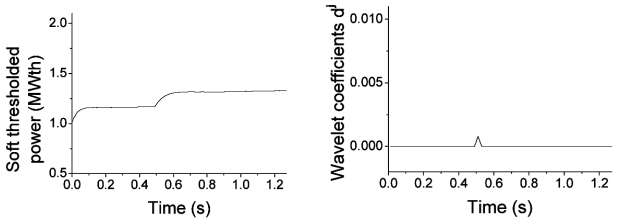

(c). Soft Thresholded Reactor Power and its Wavelet Coefficients d^1

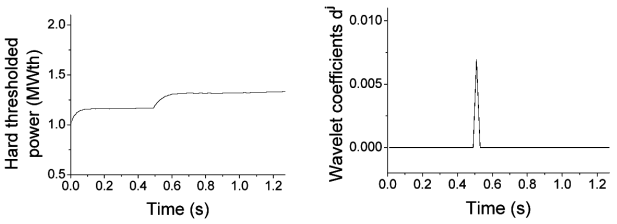

(d). Hard Thresholded Reactor Power and its Wavelet Coefficients d^1

Fig. 8. De-noised Reactor Power and its Wavelet Coefficients for the Daubechies 3 Wavelet

Fig. 9. Root-mean-square Error of a De-noised Reactor Power With Soft and Hard Thresholding

5.4 Change in the Coolant Temperature Coefficient (α_c)

The moderator (or coolant) temperature coefficient α_c could be significantly changed by variations in the boric acid concentration or the core temperature. In this simulation, α_c is assumed dropped at t=0.5sec, as shown in Fig. 10(a) under constant reactivity, and Gaussian noise $N(0,0.001^2)$ is added to the measurement. The Daubechies 3 wavelet is used to de-noise and detect the singular point. The results are presented in Figs. 10 and 11.

6. DISCUSSION

To de-noise the signal in this test, two wavelet thresholding techniques were used. The first was a hard-thresholding function and the second a soft-thresholding function. It is known that soft-thresholding is generally preferred to hard-thresholding, as the hard-thresholding function is discontinuous at $|x|=t$ in Eq.(10) [19,20]. Due to this discontinuity at the threshold, it yields abrupt artifacts in the de-noised signal, especially when the noise level is significant. However, for high frequency

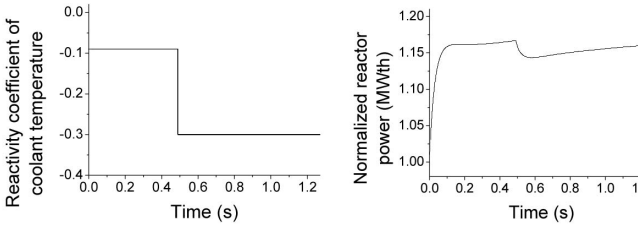

(a). Reactivity Coefficient of Coolant Temperature and Normalized Reactor Power

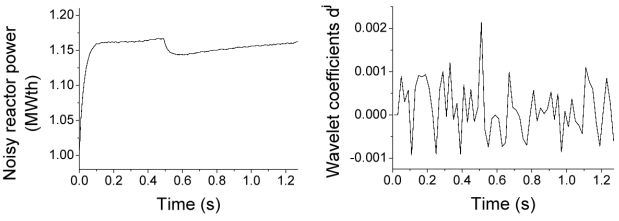

(b). Noisy Reactor Power and its Wavelet Coefficients d^1 (σ=0.001)

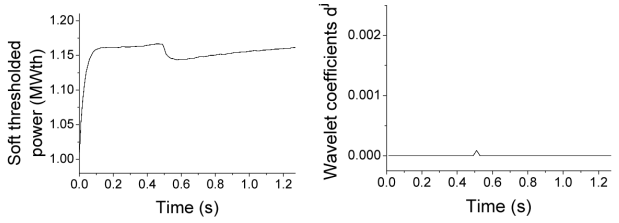

(c). Soft Thresholded Reactor Power and its Wavelet Coefficients d^1

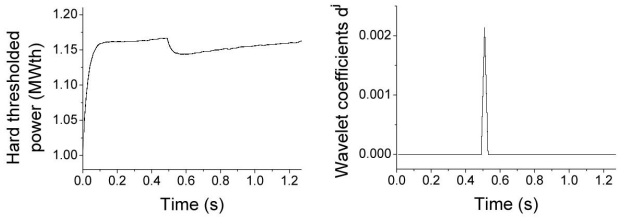

(d). Hard Thresholded Reactor Power and its Wavelet Coefficients d^1

Fig. 10. De-noised Reactor Power and its Wavelet Coefficients for the Daubechies 3 Wavelet

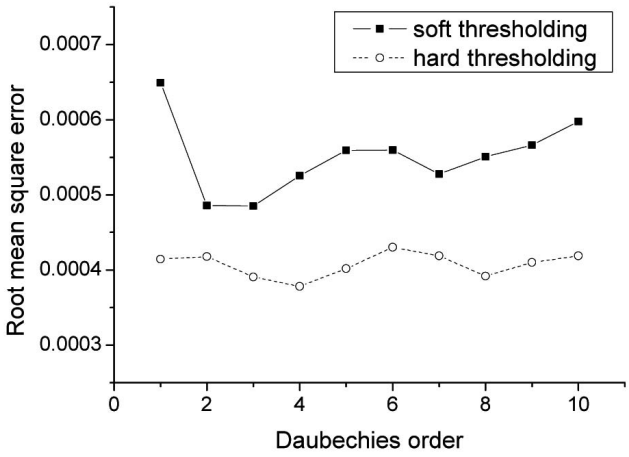

Fig. 11. Root-mean-square Error of a De-noised Reactor Power With Soft and Hard Thresholding

signals, it is clear that hard-thresholding results in superior estimates compared to those of soft-thresholding. In the test cases in this study, hard-thresholding provides smaller errors than soft-thresholding with de-noised signals, as the overall frequencies of the signals are high and broad in the temporal domain.

7. CONCLUSIONS

The investigation in this paper indicates that the wavelet transform utilizing the multiresolution property of the wavelet functions can be used to detect singularities in dynamic systems after the signal is de-noised. Numerical tests on a detailed reactor simulation model show that the changes in the reactor state as well as a change of reactivity can be detected if the singularity is not "buried" in strong noise. The wavelet transform decomposition and de-noising procedures are also shown to be computationally efficient. Thus, this wavelet theory and the wavelet functions may be profitably utilized in a real-time system for automatic event recognition (e.g., reactor condition monitoring).

ACKNOWLEDGMENTS

The authors would like to express much gratitude to the Korea Atomic Energy Research Institute for the useful information about the HANARO research reactor. This work was supported in part by the Ministry of Science and Technology of Korea through the Nuclear Technology Infrastructure and Basic Research Program.

REFERENCES

[1] I. Daubechies, "Orthonormal Bases of Compactly Supported Wavelets," *Comm. Pure. Appl. Math.*, **41**, 909 (1988).
[2] G. Strang, "Wavelets and Dilation Equations: A Brief Introduction," *SIAM Rev.*, **31**, 614 (1989).
[3] R. Glowinski, W. Lawton, M. Ravachol, and E. Tenenbaum, "Wavelet Solution of Linear and Nonlinear Elliptic, Parabolic and Hyperbolic Problems in One Space Dimension," in *Comput. Methods Appl. Sci. Eng*, SIAM, Philadelphia, 55 (1990).
[4] N. Z. Cho and C. J. Park, "Wavelet Theory for Solution of the Neutron Diffusion Equation," *Nucl. Sci. Eng.*, **124**, 417 (1996).
[5] H. Nasif, R. Omori, and A. Suzuki, "Improved Solution of the Neutron Diffusion Equation Using Wavelet Theory," *J. Nucl. Sci. Technol.*, **36** [9], 839 (1999).
[6] N. Z. Cho and L. Cao, "Wavelet-theoretic Method for Solution of Neutron Transport Equation", in Proc. *Korean Nuclear Society Spring Mtg.*, Chuncheon, Korea, CD-ROM (2006).
[7] Thie, J. A., Reactor Noise, Rowman and Littlefield, Inc, New York (1963).
[8] Thie, J. A., Power Reactor Noise, American Nuclear Society, La Grange Park, IL (1981).
[9] Uhrig, R. E., Random Noise Techniques in Nuclear Reactor Systems, The Ronald Press Company, New York (1970).
[10] Williams, M. M. R., Random Processes in Nuclear Reactors, Pergamon Press, Oxford (1974).
[11] Uhrig, R. E., "Integrating Neural Network Technology and Noise Analysis," *Progress in Nuclear Energy*, **29**, 357 (1995).
[12] Uhrig, R. E. and Tsoukalas, L. H., "Soft Computing Technologies in Nuclear Engineering Applications," *Progress in Nuclear Energy*, **34**, 13 (1999).
[13] Hines, J. W. and Uhrig, R. E., "Trends in Computational Intelligence in Nuclear Engineering," *Progress in Nuclear Energy*, **46**, 167 (2005).
[14] G. Beylkin, R. Coifman, and V. Rokhlin, "Fast Wavelet Transforms and Numerical Algorithms," *Comm. Pure. Appl. Math*, **43**, 141 (1991).
[15] S. Mallat and W.L. Hwang, "Singularity Detection and Processing with Wavelets," *IEEE Trans. Inform. Theory*, **38**, 617 (1992).
[16] D. L. Donoho, "De-noising by Soft Thresholding," *IEEE*

Trans. Inform. Theory, **41**, 613 (1995).
[17] T. W. Noh, B.S. Sim, Bo. W. Rhee, and S. K. Oh, "Korea Multipurpose Research Reactor," Korea Atomic Energy Research Institute, Tech. Rep. KM-031-400-02 (1989).
[18] C. J. Park and N. Z. Cho, "Reactor Condition Monitoring via Wavelet Transform De-noising," in Proc. *Korean Nuclear Society Autumn Mtg*., Daejeon, Korea, 67 (1996).
[19] B. J. Yoon and P. P. Vaidyanathan, "Wavelet-based Denoising by Customized Thresholding," in *Proc. 29th IEEE Int. Conf. Acoustics, Speech, and Signal Processing*, **2**, 925 (2004).
[20] S. G. Chang, B. Yu, and M. Vetterli, "Adaptive Wavelet Thresholding for Image Denoising and Compression," *IEEE Trans. Image Processing*, **9**, 1532 (2000).